Theory of segregation using the equivalent-medium approximation and bond-strength modifications at surfaces: Application to fcc Pd-*X* alloys

J. L. Rousset,* J. C. Bertolini, and P. Miegge
Institut de Recherches sur la Catalyse, CNRS, 2 avenue A. Einstein, F69626, Villeurbanne CEDEX, France
(Received 18 September 1995)

We have developed, in the framework of a broken-bond model, a method to determine the surface composition of transition metal alloys. The model is based on the equivalent-medium approximation which allows us to calculate the energies of surface layers as a function of local concentration. The model also considers bond strength modifications at the surface that are determined within a modified tight-binding scheme. The model has been applied to several fcc Pd-based alloys. The results are found to be in good agreement with available experimental data.

I. INTRODUCTION

A detailed knowledge of chemical composition at surfaces of alloys is of primary importance in the field of catalysis and corrosion. Surface segregation of bimetallic alloys opens the way to a new generation of catalysts with tuned surfaces highly concentrated in the active component for a given reaction, even for low bulk concentration. Since Pd is a very good catalyst for hydrogenation reactions, we have been motivated to study in our laboratory the segregation and catalytic properties of some of the Pd-based alloys. Recently, we have found from low-energy ion scattering (LEIS) experiments that for Pd_1Ni_{99} and Pd_5Ni_{95} alloys, Pd concentration in the top layer reaches as high as 20% and 50%, respectively.[1] For Pd_1Fe_{99} alloy, LEIS experiment shows that the top layer Pd concentration is almost 50%.[2] LEIS has also shown a slight Cu segregation for (111) orientation in the $Pd_{50}Cu_{50}$ single-crystal system.[3] Again, for the $Pd_{65}Pt_{35}$ alloy we have found indication of large Pd segregation to the surface.[4] In order to get a better understanding of the experimental results, mainly for systems undergoing very large surface segregation, we have developed a model that we present in this paper. The model uses the concept of equivalent medium approximation (EMA), which allows us to calculate concentration-dependent pair interactions. Bond-strength modifications at surfaces are taken into account through an empirically modified tight-binding scheme in the second moment approximation (MTB). This model includes elastic strain effects for alloys constituted by elements of different sizes. From the thermodynamic data of pure metals and bulk alloys we have been able to predict semiquantitatively the composition of the top five layers. The plan of the paper is as follows.

In Sec. II we present our model. The model is general and can be applied, in principle, to all transition and noble metal alloys. However, in this paper we apply the model to study the segregation behavior of a few Pd-based systems. The results are presented in Sec. III. Conclusions are drawn in Sec. IV.

II. FORMULATION OF THE MODEL

Let us consider a semi-infinite solid binary alloy A_xB_{1-x} in thermodynamic equilibrium (Fig. 1). Only the compositions of the five top layers are allowed to differ from the bulk value. The assumption of a disordered alloy is made. Moreover, the study is here limited to fcc alloys for which only interactions with first nearest neighbors are considered according to the standard approximation.

Let us define the free enthalpies G_s and G_b associated, respectively, with the five surface layers and with the bulk. The total free enthalpy of the system is

$$G_t = G_s + G_b, \tag{1}$$

where $G_s = H_s - TS_s$ and $G_b = H_b - TS_b$, H and S being, respectively, the enthalpy and the entropy; T is the temperature.

A. Treatment of the bulk alloy

In the bulk of the pure metal A, the interatomic equilibrium distance is $R^0_{AA} = 2R_A$ (R_A being the atomic radius). The bond enthalpy, ε^0_{AA}, is related to the sublimation enthalpy with the classical relation

$$\varepsilon^0_{AA} = -2\Delta H_{\text{sub}}/Z, \tag{2}$$

where Z is the coordination number in the bulk and ΔH_{sub} is the enthalpy of sublimation. For the alloy A_xB_{1-x}, one has to

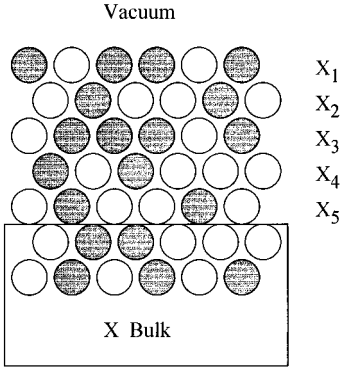

FIG. 1. Schematic drawing representing the semi-infinite alloy considered for the calculations. Five layer concentrations have been allowed to differ from the bulk one.

define a new equilibrium distance R_{alloy}, which depends on the concentration. The strain energy that results from compression or expansion (depending on the atomic radius of the components) may be taken into account through pairwise Lennard-Jones (LJ) potential. The energies ε_{AA} (similarly ε_{BB}) are then written as[5–8]

$$\varepsilon_{AA}(X)=\varepsilon^0_{AA}\psi_{AA}(X), \tag{3}$$

with

$$\psi_{AA}(X)=2\left(\frac{R^0_{AA}}{R_{\text{alloy}}(X)}\right)^6-\left(\frac{R^0_{AA}}{R_{\text{alloy}}(X)}\right)^{12}, \tag{4}$$

where X is the concentration of the A component.

Similarly, the effective bond enthalpy ε_{AB} between A and B atoms of the alloy may be calculated as

$$\varepsilon_{AB}(X)=\varepsilon^0_{AB}\psi_{AB}(X), \tag{5}$$

with

$$\psi_{AB}(X)=2\left(\frac{R^0_{AB}}{R_{\text{alloy}}(X)}\right)^6-\left(\frac{R^0_{AB}}{R_{\text{alloy}}(X)}\right)^{12}, \tag{6}$$

where $R^0_{AB}=R_A+R_B$ and ε^0_{AB} is related to the mixing enthalpy ΔH_m. But the mixing enthalpy is given by

$$\Delta H_m=H_2-H_1, \tag{7}$$

where

$$H_1=\tfrac{1}{2}XZ\varepsilon^0_{AA}+\tfrac{1}{2}(1-X)Z\varepsilon^0_{BB}\quad\text{(enthalpy before mixing)}, \tag{8}$$

$$H_2=\tfrac{1}{2}X^2Z\varepsilon^0_{AA}\psi_{AA}(X)+X(1-X)Z\varepsilon^0_{AB}\psi_{AB}(X)+\tfrac{1}{2}(1-X)^2Z\varepsilon^0_{BB}\psi_{BB}(X) \tag{9}$$

(solution enthalpy after mixing)

With the values of the bond enthalpies ε^0_{AA} and ε^0_{BB} from sublimation enthalpies of pure metals, and ε^0_{AB} from the variation of ΔH_m with concentration X,[9] one may calculate the bulk free enthalpy G_b as

$$G_b=Z[\tfrac{1}{2}X_b^2\varepsilon^0_{AA}\Psi_{AA}(X_b)+X_b(1-X_b)\varepsilon^0_{AB}(X_b)\Psi_{AB}(X_b)+\tfrac{1}{2}(1-X_b)^2\varepsilon^0_{BB}\Psi_{BB}(X_b)]+RT[X_b\ln(X_b)+(1-X_b)\ln(1-X_b)]. \tag{10}$$

B. Treatment of the surface layers

The model described in Sec. II A has been used even for surfaces in several studies.[7–8] But this approach has some serious problems. First of all, the value of $\varepsilon_{AB}(X)$ is calculated for an arbitrary bulk concentration value and it is not readjusted for the surface layers when changes in concentration occur. This is especially problematic in the case of strong segregation. Secondly, a relaxation parameter has to be empirically introduced to account for the lack of bonds at the surface (the remaining bonds being reinforced). It is in fact adjusted such as to fit with experimental results.[7] We consider these points in the following subsections.

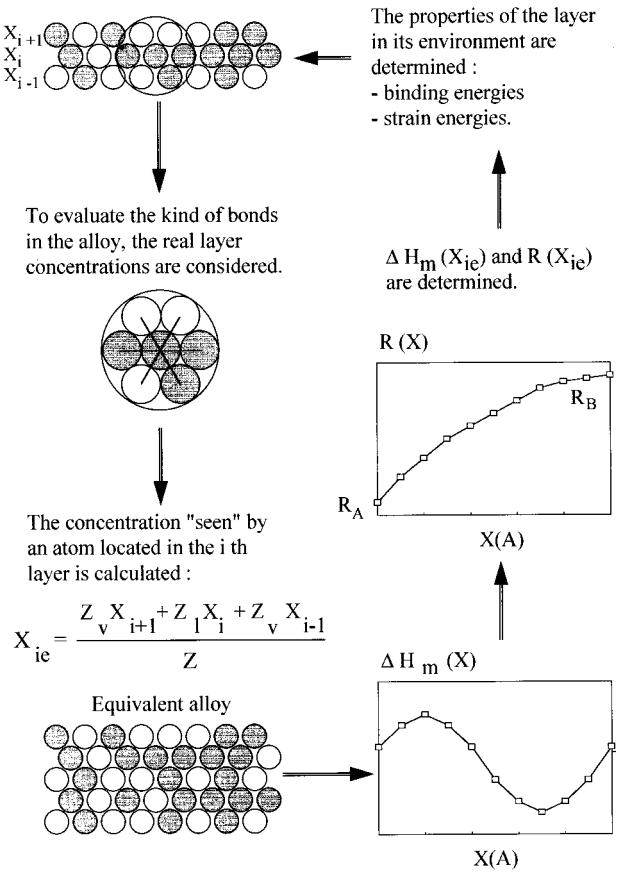

FIG. 2. Representation of the equivalent medium approximation (EMA) cycle used in the calculations for an alloy AB. At each step of the segregation process, the (local) equivalent concentration in which the considered atom is embedded is evaluated and corresponding properties are determined.

1. The equivalent medium approximation (EMA)

For the surface region one has to take into account the thermodynamic properties of atoms in their local environment, which changes when the segregation process is occurring. One way to do that would be to reevaluate the pair interactions $\varepsilon_{AA},\varepsilon_{BB},\varepsilon_{AB}$ for a concentration equivalent to that of the considered layer: $X_1,X_2,\ldots,X_i$. For the atoms in one layer, this would be equivalent to ignoring the influence of the adjacent layers, which would be erroneous particularly in the case of oscillating profiles. A more satisfying approach may be proposed as follows: let us consider an atom located in the ith surface layer with concentration X_i as described in Fig. 2. This atom is surrounded by the layer $i-1$ with concentration X_{i-1} and the layer $i+1$ with concentration X_{i+1}. In the disordered state one can consider that this atom is *embedded in an equivalent medium* with concentration X_{ie} given by

$$X_{ie}=\frac{Z_v}{Z}X_{i-1}+\frac{Z_l}{Z}X_i+\frac{Z_v}{Z}X_{i+1}, \tag{11}$$

where Z_v is the number of vertical bonds between two adjacent layers; Z_l is the number of lateral bonds in each layer, and Z is the total coordination number.

TABLE I. Values of calculated TB-SMA parameters A (eV), ξ (eV), and p, and q for fcc transition and noble metals. (a) Calculated values, (b) experimental values of r_0 (Å), E_c (eV) (from Ref. 12) and elastic constants (Mbar) C_{11}, C_{12}, C_{44}, C', C_{44} and bulk modulus B (from Ref. 13).

		Ni	Pd	Pt	Cu	Ag	Au
	ξ	1.5066	1.8194	2.6572	1.4125	1.3396	1.8986
	A	0.0653	0.1972	0.2793	0.1124	0.1401	0.2331
	p	13.18	10.44	10.71	9.83	9.83	9.92
	q	1.98	3.92	3.90	2.71	3.56	4.22
$-E_c$	(a)	4.435	3.936	5.853	3.544	2.960	3.779
	(b)	4.435	3.936	5.853	3.544	2.960	3.779
R_0	(a)	2.491	2.749	2.775	2.556	2.889	2.884
	(b)	2.491	2.749	2.775	2.556	2.889	2.884
C_{11}	(a)	2.65	2.34	3.49	1.86	1.31	1.87
	(b)	2.61	2.34	3.58	1.76	1.31	1.87
C_{12}	(a)	1.49	1.76	2.57	1.20	0.96	1.55
	(b)	1.51	1.76	2.54	1.25	0.97	1.55
C_{44}	(a)	1.16	0.58	0.92	0.66	0.35	0.32
	(b)	1.32	0.71	0.77	0.82	0.51	0.45
C'	(a)	0.58	0.29	0.46	0.33	0.18	0.16
	(b)	0.55	0.29	0.52	0.26	0.17	0.16
B	(a)	1.88	1.95	2.88	1.42	1.08	1.66
	(b)	1.88	1.95	2.88	1.42	1.08	1.66

Then, one can determine the different parameters, for each layer i, by taking into account the *equivalent* concentration X_{ie} and the corresponding values of the enthalpy of mixing and lattice parameter. So we will have to consider for the layer i the parameters $R_{\text{alloy}}(X_{ie})$, $\psi_{AA}(X_{ie})$, $\psi_{BB}(X_{ie})$, $\psi_{AB}(X_{ie})$, $\Delta H_m(X_{ie})$ only. As a consequence, the pair potential interactions will be different from one layer to the others. This approach appears to be well adapted for solutions far from regular ones. However, even in the case of a *regular* solution, potential interactions are varied with concentration because of the LJ potential terms and need to be calculated in the framework of the EMA approach. But it is not well suited when the atomic coordination number changes, i.e., for the top surface atoms. For the top layer we have to consider an additional modification due to lower coordination number, which give rise to bond relaxation. This is discussed in the following subsection.

2. Bond-strength modifications at surfaces and bond relaxation parameters

In the broken-bond model a relaxation parameter has to be introduced. It is a number that multiplies the bond enthalpies for surface atoms with respect to the bulk ones and can be generally expressed as

$$(1+\delta)\varepsilon^{\text{bulk}}=\varepsilon^{\text{surface}} \tag{12}$$

where δ is the relaxation parameter and $\varepsilon^{\text{bulk}}$ and $\varepsilon^{\text{surface}}$ are, respectively, the bulk and surface bond energies.

This parameter δ reflects the modifications of bond strengths due to the changes of the coordination number for the surface sites. In order to derive such a parameter at first we have to evaluate the surface site energies.

To do this we have used the tight-binding scheme in the second moment approximation (TB-SMA).

In this scheme the band energy of an atom i can be written as[10,11]

$$E_b^i=-\left\{\sum_j \xi^2\exp[-2q(r_{ij}/r_0-1)]\right\}^{1/2}, \tag{13}$$

where ξ is an effective hopping parameter, r_{ij} is the distance between atom i and j, and r_0 is the distance between next-nearest neighbors. For the repulsive energy to be added to ensure equilibrium, a pairwise Born-Mayer-type potential is assumed:[10,11]

$$E_r^i=\sum_j A\ \exp[-p(r_{ij}/r_0-1)]. \tag{14}$$

TABLE II. Calculated (using TB-SMA) and experimental values for the surface tensions. The experimental values are from Tyson and Miller (Ref. 14).

	Ni	Pd	Pt	Cu	Ag	Au
$\sigma(111)$ (mJ m^{-2})	1498	618	949	900	446	404
$\sigma(100)$ (mJ m^{-2})	1796	779	1189	1097	558	528
$\sigma(110)$ (mJ m^{-2})	1938	860	1309	1194	615	592
Experimental (mJ m^{-2})	2380	2005	2490	1790	1245	1505

TABLE III. Values of $f(1)$, $f(8)$, and $f(11)$ using Eqs. (18), (19), and (20) and experimental data of D_0, E_v, and σ, respectively from Refs. 16, 17, and 14 (see text).

	Ni	Pd	Pt	Cu	Ag	Au
D_0 (eV)	2.37	1.09	2.90	2.03	1.66	2.28
σ (eV/atom)	0.92	0.95	1.20	0.73	0.65	0.78
E_v (eV/atom)	1.50	1.26	1.35	1.17	1.10	0.95
$f(1)$	0.8299	0.4107	0.6508	0.7982	0.7241	0.7233
$f(8)$	0.9475	0.8876	0.9164	0.9295	0.9053	0.9058
$f(11)$	1.0064	0.9944	1.0000	0.9997	0.9923	0.9949
α	0.8154	0.3165	0.6048	0.7832	0.7007	0.7001
β	0.01 425	0.0974	0.04 701	0.01 458	0.02 308	0.02 281
γ	0.000 2833	−0.003 253	−0.00 101	0.000 464	0.000 311	0.000 363

Then the cohesive energy of the atom i is

$$E_c^i = E_b^i + E_r^i. \tag{15}$$

Thus, the cohesive energy depends on four parameters A, ξ, p, and q. By taking the right derivatives of this energy with respect to the components of the deformation,[12] one gets relations between elastic constants and these parameters (see Appendix A). The TB-SMA parameters, extended only to first-nearest neighbors, have been calculated. They are presented in Table I together with the calculated and the experimental values of E_c, r_0, C_{11}, C_{12}, C_{44}, and bulk modulus B. If we define $E(Z)$ as the energy of an atom having Z nearest neighbors we can write the following expressions for the surface tension of (111), (100), and (110) surfaces:

$$\sigma(111) = E(9) - E(12) \quad \text{(a)},$$

$$\sigma(100) = E(8) - E(12) \quad \text{(b)}, \tag{16}$$

$$\sigma(110) = E(7) + E(11) - 2E(12) \quad \text{(c)}.$$

The values of σ for different orientations are presented in Table II together with experimental average surface tensions. It may be noticed that the agreement between the calculated and the experimental values is not good. This is because ξ and A (which are evaluated using bulk constants) are assumed to be independent of the coordination number in the TB-SMA scheme. However, for going from bulk to surface one should take into consideration the intra-atomic charge transfer between d and s-p electrons in the valence band. This influences the site energies. In order to find the site energies we develop a MTB approach where we empirically modify the hopping parameter as

$$\xi(Z) = f(Z)\xi. \tag{17}$$

Here ξ has the values given in Table I and $f(Z)$ is an empirical function, which has to be determined. Charge transfer does not affect too much the repulsive parameter A as is generally assumed.[15] To determine this function $f(Z)$ we used the experimental values of the surface tension σ [assumed to be that of the (100) face having the mean atomic density with respect to (111) and (110) faces], the homonuclear dimer bonding energy D_0, and the bulk monovacancy formation energy E_v.

The following equations may be derived from Eq. (15):

$$D_0/2 = E(1) = f(1)\xi + A, \tag{18}$$

$$\sigma = E(8) - E(12) = E_c + [f(8)\sqrt{8}\xi - 8A], \tag{19}$$

$$E_v = 12[E(11) - E(12)] \Rightarrow E_v/12 = E_c + [f(11)\sqrt{11}\xi - 11A], \tag{20}$$

with $f(12) = 1$ by definition. If one assumes that $f(Z)$ may be described by a polynomial of second order as

$$f(Z) = \alpha + \beta Z + \gamma \cdot Z^2, \tag{21}$$

one can deduce the three constants α,β,γ (see Table III) and obtain a corrective curve $f(Z)$ for all the Z values (from 1 to 12 for fcc metals). $f(1)$, $f(8)$, and $f(11)$ values are also provided in Table III. $f(Z)$ versus Z curves are shown in Fig. 3 for several metals. It may be noticed how this parameter varies with Z compared to the TB-SMA situation where $f(Z)$ is constant. Going over to the cohesive energy $E(Z)$ of an atom as a function of Z, the results for Ni and Pd are given, respectively, in Figs. 4 and 5. For Ni one can see that the two curves derived from MTB and TB-SMA calculations are very similar. However, quantitative discrepancies occur for all Z values and increase when the coordination number de-

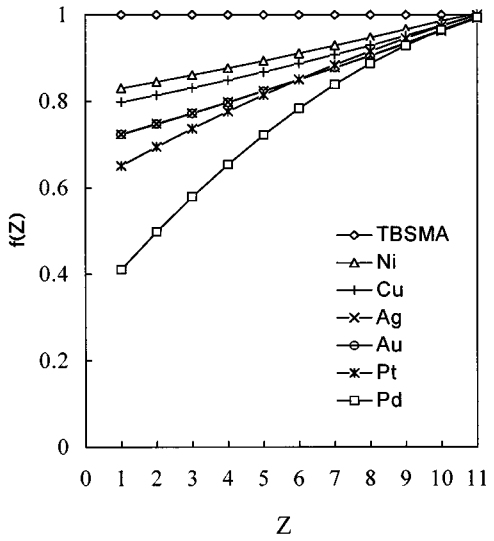

FIG. 3. Calculated corrective curves $f(Z)$ of site energies for selected elements.

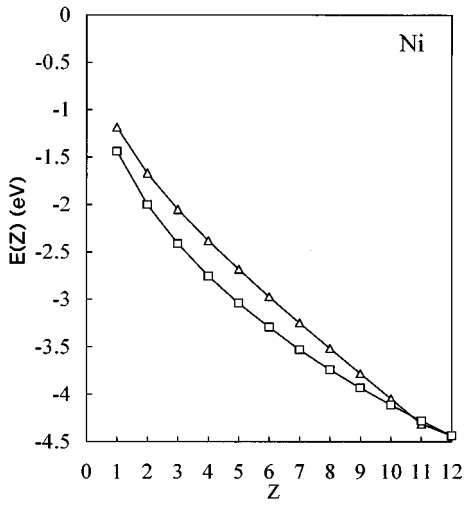

FIG. 4. Cohesive energy $E(Z)$ per nickel atom, as a function of coordination: evaluations from TB-SMA (□) and MTB (△) models.

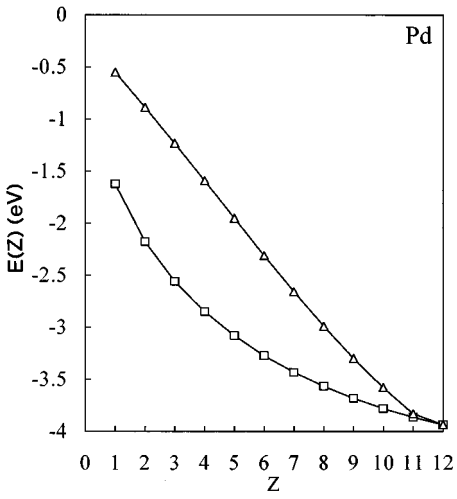

FIG. 5. Cohesive energy $E(Z)$ per palladium atom, as a function of coordination: evaluations from TB-SMA (□) and MTB (△) models.

creases. Concerning Pd metal, very large differences between TB-SMA and MTB results exist in the whole coordination range. This could be due to large reconfiguration and s-d hybridization. This is very important for the study of segregation processes for surfaces exhibiting low coordinated sites: steps, kinks, or small particles. The TB-SMA model is qualitatively correct but only approximate when accurate evaluations of site energies are needed. The MTB model, which is developed here for the study of surface segregation, could be used in every study for which site energies are needed. Indeed, the MTB model has been successfully applied to the determination of the equilibrium shape of small bimetallic Pd-Pt clusters obtained by low energy cluster beam deposition.[4] It is now easy to derive the relaxation parameter, $\delta^{Z,Z'}$, for different surface orientations, from the site energies calculated in the framework of the MTB model. Let π_A^Z be the partial energetic contribution to a simple bond of an atom of type A with Z nearest neighbors.[18] The cohesive energy (or site energy) of this atom is $E(Z)=Z\pi_A^Z$. In the same way, $\pi_A^{Z'}$ is the energetic contribution of another atom of element A with Z' nearest neighbors and $Z'\pi_A^{Z'}$ is the cohesive energy of that atom. The bond enthalpy between these two atoms in pure metal A is then

$$\varepsilon_{AA}^{Z,Z'}=\pi_A^Z+\pi_A^{Z'}, \tag{22}$$

A schematic representation of the interactions for surface atoms belonging to a (111)-oriented single crystal is shown in Fig. 6.

The relaxation parameter $\delta^{Z,Z'}$ is defined by the relation

$$1+\delta^{Z,Z'}=\frac{\pi^Z+\pi^{Z'}}{2\pi^{12}} \tag{23}$$

and each bond energy in the top surface layer will be the product of the corresponding bulk bond enthalpies by $(1+\delta^{Z,Z'})$.

For bonds between first and second layers we have to take into account $(1+\delta^{Z,Z'}/2)$. In order to calculate $\delta^{Z,Z'}$ for heteronuclear bonds in the alloys it is assumed that the mixing enthalpy divided by the coordination number is a constant and one can write

$$1+\delta_{AB}^{Z,Z'}=\frac{\Delta H_m(X_{1e})-0.5X_{1e}\varepsilon_{AA}^0 Z(1+\delta_{AA}^{Z,Z'})[X_{1e}\Psi_{AA}(X_{1e})-1]-0.5X_{1e}\varepsilon_{BB}^0 Z(1+\delta_{BB}^{Z,Z'})[X_{1e}\Psi_{BB}(X_{1e})-1]}{ZX_{1e}(1-X_{1e})\varepsilon_{AB}^0(X_{1e})\psi_{AB}(X_{1e})}. \tag{24}$$

In fact, the δ_{AB} values are found nearly equal to the arithmetic mean value of δ_A and δ_B irrespective of the concentration of the alloy. Figure 7 shows the different relaxation parameters considered in this study. We notice that when a surface atom A (B) is bonded with a B (A) atom in the second layer only the ability of the surface A (B) atom to release energy (i.e., δ_A) is taken into account. One also has to emphasize that π^Z are calculated for pure metals and consequently give relaxation parameters for pure elements. For coherence with the EMA, which already includes strain effects in the alloy, we need to eliminate size effects in the determination of the relaxation parameters. So, to calculate δ_A and δ_B for the considered alloy AB, we assume A and B atoms to have the same radius corresponding to the mean value of the radii of A and B components.

One can now express the total free enthalpy of the system by considering the summation of all the pair interactions in the five surface layers (with the respective composition X_1, X_2, X_3, X_4, and X_5) (see Appendix B). From total free en-

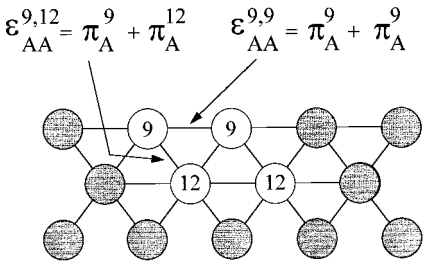

FIG. 6. Schematic relation between bond energy ($\varepsilon_{AA}^{Z;Z'}$) and partial bond energy (π_A^Z) as defined in the text after Donnelly and King (Ref. 18). The scheme is reported for (111) orientation of (pure) metal A.

thalpy and its derivative one can now get the surface layer concentrations corresponding to the equilibrium state of the system.

III. APPLICATIONS

The segregation behavior of several fcc Pd-based alloys has been studied in this work. The first layer composition and layer-by-layer depth profiles have been calculated in the whole concentration range and for two surface orientations, (100) and (111). For all the alloys studied in this work, the experimental mixing enthalpies and cell parameters have been taken from Refs. 9 and 19, respectively, except for the Pd-Pt alloy for which values from Ref. 20 have been used.

A. Pd-Ni

We have studied experimentally Pd-Ni alloys in our laboratory. Pd segregates to a large extent on Pd_1Ni_{99} and Pd_5Ni_{95} polycrystalline samples as determined from LEIS experiments.[1] Experimental and calculated results concerning the first layer composition of the Pd-Ni system are shown in Fig. 8. A strong segregation is evidenced for all the considered faces. It is more pronounced for very diluted alloys. The agreement between theory and experiment is quite good. Concerning the concentration profile, the results are more complex. It is important to point out that Pd-Ni is an endothermic system for Pd concentration up to 0.4, but becomes exothermic for higher Pd concentrations. This implies an irregular mixing enthalpy for this alloy.[9] The calculated profiles reported in Figs. 9(a) and 9(b) show a strong dependence on concentration. Whatever may be the concentration,

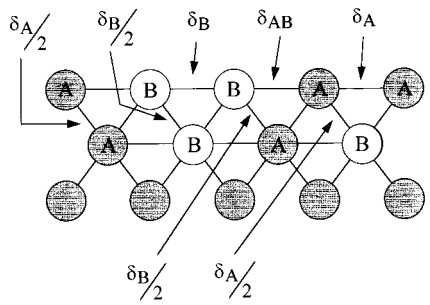

FIG. 7. Relaxation parameters used in the calculations: the bonds are those of a hypothetical alloy AB.

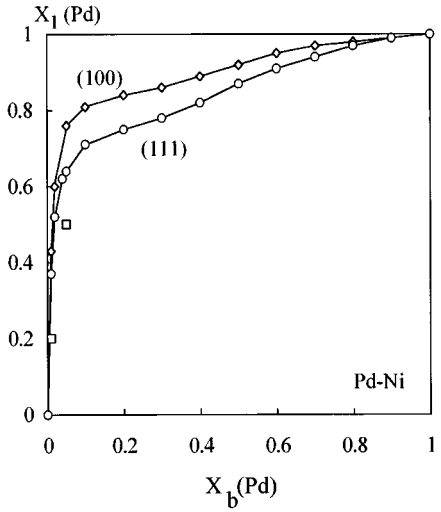

FIG. 8. Composition of the first atomic layer of (111) (○) and (100) (◇) orientations of Pd-Ni alloys calculated at 800 K. The squares (□) represent values deduced from ion scattering obtained for the surface composition of polycrystalline samples.

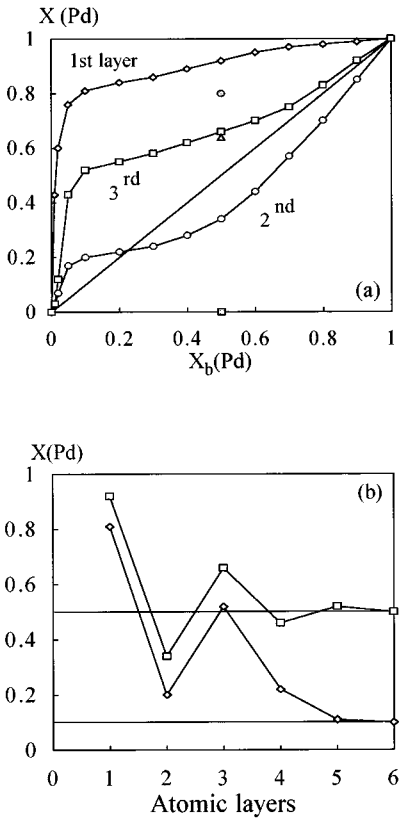

FIG. 9. (a) Composition in the first (◇), second (○), and third (□) atomic layers of the (100) surface of Pd-Ni calculated at 800 K. The shaded circle, square, and triangle represent, respectively, the first, second, and third layer concentrations deduced from LEED measurements on (100) surface of a single-crystal $Ni_{50}Pd_{50}$ alloy (Ref. 21). (b) Composition depth profiles calculated for Pd-Ni alloys at 800 K for 0.1 and 0.5 bulk Pd concentration.

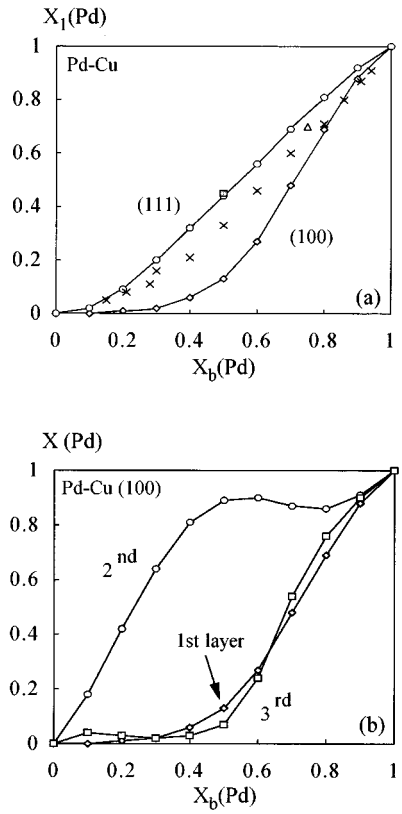

FIG. 10. (a) Same as Fig. 8 for the Pd-Cu alloy at 800 K. The crosses (×) represent Auger results for the surface composition of a polycrystalline sample equilibrated at 670 K from Ref. 22. The square represents the ion scattering result of a (111)-oriented alloy from Ref. 3 and triangle is the Auger result obtained for (111)-oriented alloy from Ref. 23. (b) Composition in the first (◇), second (○), and third (□) atomic layers of the (100) surface of Pd-Cu calculated at 800 K.

the profile is oscillating. In the case of high bulk Pd concentration (>0.5) there are oscillations of mean amplitude and the calculated profile is coherent with a negative mixing enthalpy. Indeed, unlike atoms prefer to be adjacent in an exothermic alloy. These results are consistent, at least qualitatively, with those obtained experimentally by Derry, McVey, and Rous for the (100) surface of a single-crystal $Pd_{50}Ni_{50}$ alloy.[21] These authors found oscillating depth profile up to the third layer as shown in Fig. 9(a). For low bulk Pd concentration, the Pd segregation is very high and oscillations around a composition higher than the bulk one are observed [see Fig. 9(b)]. This corresponds to the formation, in the near surface region, of a highly Pd-concentrated alloy, i.e., an exothermic alloy. This could explain the appearance of oscillations around a mean concentration value higher than the bulk one but which decrease faster with depth.

B. Pd-Cu

The results for Pd-Cu are given in Fig. 10. Firstly, a relatively strong orientation effect on surface segregation is observed. The (111) top layer composition is found to be close to the bulk one in the whole composition range, while strong Cu segregation is found for the (100) orientation. Experimentally, the surface region of polycrystalline Pd-Cu equilibrated at 670 K (Ref. 22) is found to be enriched in copper with X(Pd) values lying between the theoretical curves for (100) and (111) orientations. LEIS study that we performed on a (111)-oriented monocrystalline $Pd_{0.5}Cu_{0.5}$ alloy gave results [shown in Fig. 10(a)] in very good agreement with our model calculations. Also interesting are the depth profiles for this system. Phase diagram and thermodynamical data[9] indicate that the Pd-Cu alloy has a highly negative mixing enthalpy, i.e., it is strongly exothermic. Moreover, ordered phases have been observed for Pd content smaller than 0.55. For example, in the bulk phase $Pd_{0.5}Cu_{0.5}$, a transition between an ordered bcc structure (isotopic with CsCl) and a disordered fcc phase is observed at a critical temperature $T_c = 780$ K. In Fig. 10(b) are displayed surface versus bulk Pd compositions for some layers. The temperature at which the calculation was made, 800 K, is very close to the bulk ordering temperature T_c. Clearly, one can see a direct relation between the oscillatory profile of the (100) face and bulk ordering [Fig. 10(b)]. For Pd concentrations smaller than about 0.5 one observes very large oscillations, which can be viewed as *surface preordering*.[24] For larger Pd concentrations, the oscillations decay more quickly with depth toward the nominal composition. This is consistent with the lack of order disorder transition for such bulk concentration.

C. Pd-Pt

This system illustrates the surface behavior of a nearly regular exothermic alloy with low heat of mixing and for which no strong size (strain) effects are expected since the atomic radii of the two components are rather similar (1.5% mismatch). The calculated top layer concentrations are presented in Fig. 11(a). A strong Pd segregation is found for both orientations. Calculated results for depth profiles up to the third layer are shown in Fig. 11(b) for a (100) surface. For such a system, the depth profile behavior is very "simple," as expected. We observe damped oscillations in the whole composition range. The bulk composition is nearly reached for the third atomic layer.

D. Pd-Au and Pd-Ag alloys

For Pd-Au, the top layer is found to be enriched in Au for both faces as shown in Fig. 12(a). LEIS experimental results for a polycrystalline sample equilibrated at 873 (Ref. 25) and 773 K (Ref. 26) are also indicated. These experimental results lie between calculated values for (100) and (111) orientations. Segregation is again rather well predicted. The system presents a quasimonolayer segregation for the (111) orientation, and the underlayer is calculated to have a composition very close to the bulk one. The (100) orientation exhibits larger oscillations, as expected. The oscillations are present in the whole concentration range and no peculiar features are noticed. The results for Pd-Ag are rather similar to those of Pd-Au. Strong face effects are evidenced (Fig. 13) and the same kind of in-depth profiles are calculated. The Ag segregation is, however, more pronounced, which agrees well with Auger experimental results by Kuijers and Ponec[27] on polycrystalline samples equilibrated at 673 K.

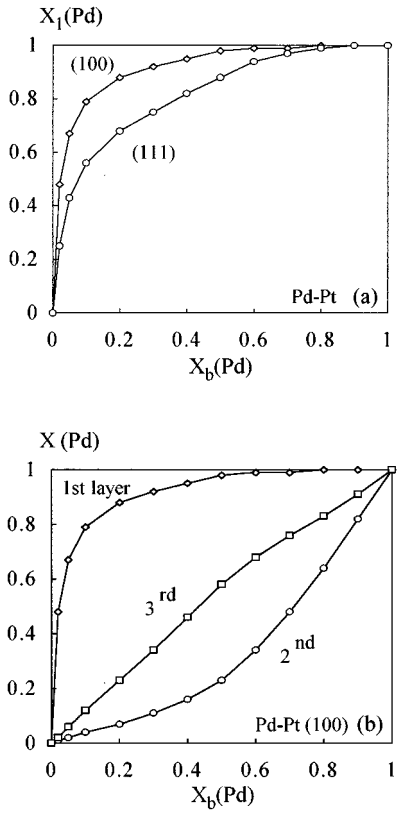

FIG. 11. (a) Composition in the first atomic layer of (111) (○) and (100) (◇) surfaces of Pd-Pt, as computed for 800 K. (b) Calculated in-depth Pd concentrations versus bulk concentration at $T=800$ K for the (100) Pd-Pt surface. The Pd concentration of the first (◇), second (○), and third (□) layers are represented.

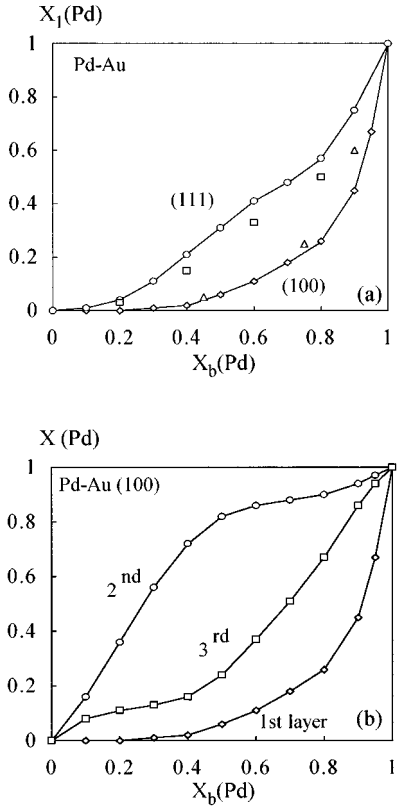

FIG. 12. (a) Same as Fig. 11(a) for Pd-Au at 800 K. The squares (□) and the triangles (△) are ion scattering results for polycrystalline samples equilibrated, respectively, at 873 K (Ref. 25) and 773 K (Ref. 26). (b) Same as Fig. 11(b) for Pd-Au alloy.

E. Contribution of the EMA approach

It will be appropriate now to discuss the contribution of the EMA approach to the determination of both the top layer concentration and the depth profiling. To illustrate this, we have chosen the Pd-Cu system. We compare the results obtained with the EMA approach with those derived from the basic model where parameters ε^0_{AB}, $\Delta H_m(X)$, $R_{al}(X)$, $\psi_{AA}(X)$, $\psi_{BB}(X)$, $\psi_{AB}(X)$ etc. are the same for bulk as well as surface layers. The results are obtained for a nominal composition of 0.5, for which there is an order-disorder transition at $T_c=780$ K in the bulk phase[9] and are compared in Fig. 14 for three different temperatures.

Please note, the top layer concentrations calculated by the two approximations are very close. This is because bond strength modifications at the very surface are the leading force of segregation to the top layer. Above T_c, the equilibrium depth profiles, however, depend on the approximation used in the calculation. The basic model leads to very large oscillations for both 1000 and 1500 K, while the EMA leads to damped profiles and the magnitude of the oscillations decreases strongly with increase in temperature. The later profiles are expected at $T>T_c$ for exothermic alloys. Below T_c, EMA leads to weakly damped oscillations. Once again the basic approach gives very strong oscillations. We have to emphasize, however, that for temperature below T_c, both calculations (basic model and EMA) are not rigorous. Indeed, the bulk free enthalpy is calculated assuming a disordered state even though the phase diagram presents an ordered phase. Moreover, this ordered phase has a bcc structure. Nevertheless, the calculations give indications of consistency in the determined profiles, at least qualitatively. We observe that EMA gives profiles whose evolution with temperature is very satisfying: damped oscillations for $T>T_c$ and marked ordering tendency for $T<T_c$. Indeed, it may be noticed that for the (100) orientation, the ordered bcc phase (Pd-Cu) would show alternate pure Pd and Cu planes. The environment of each Pd (Cu) atom in the bcc ordered structure consists of eight nearest neighbors of the other species and six second neighbors of the same species. However, for the bcc structure the second-neighbor distance is of the order of 1.15 times the distance of the first-nearest neighbor. The present model, which treats the Pd-Cu as the fcc structure even below the order-disorder temperature, gives nearly alternate of pure Pd or Cu layers. The environment of each Pd (Cu) atom here consists of eight atoms of the other species and four atoms of the same species. The results obtained from our model, as shown in Fig. 14(c), very closely mimic the ordered bcc phase, as expected.

The same kind of argument holds also for Pt-Cu and Au-Cu systems for which calculations have also been done. A large enhancement of oscillations is found in going from a temperature above T_c to a temperature below T_c with EMA while the basic model approximation leads always to very large oscillations at all temperatures. Once again, the profile

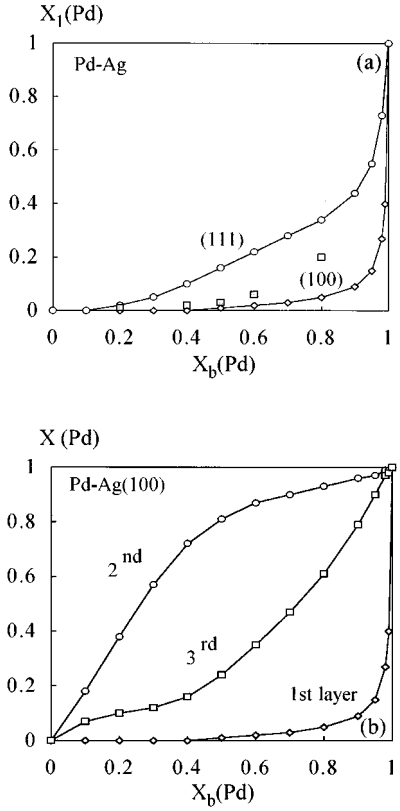

FIG. 13. (a) First atomic layer composition of (111) (○) and (100) (◇) surfaces of Pd-Ag, as calculated for $T=800$ K. The squares (□) represent Auger results by Kuijers and Ponec (Ref. 27) on polycrystalline samples equilibrated at 673 K. (b) Calculated in-depth Pd concentrations versus bulk concentration at $T=800$ K for the (100) Pd-Ag surface. The Pd concentration of the first (◇), second (○), and third (□) layers are represented.

determined using the EMA approach appears to be the more convincing, especially when evolution with temperature is concerned.

IV. SUMMARY AND CONCLUSION

A thermodynamical approach is proposed that overcomes two main problems encountered with simple bond-breaking theory: (i) energetic parameters such as bond strengths are usually calculated for a given bulk concentration and they are kept constant up to the surface; (ii) bond strengths or site energy modifications accompanying the changes in coordination number are evaluated either fitting empirically with the experimental results or by using models such as the embedded atom method or tight-binding model in the second moment approximation, which do not give satisfying quantitative results.

The equivalent medium approximation, which allows us to calculate the energetics of the surface layers as a function of the local concentration, solves the first problem. With respect to the second one, the *qualitatively* meaningful tight-binding model in the second moment approximation has been modified in order to derive *quantitative* bond-strength values. This empirical modification is clearly related to reconfiguration and rehybridization processes happening when

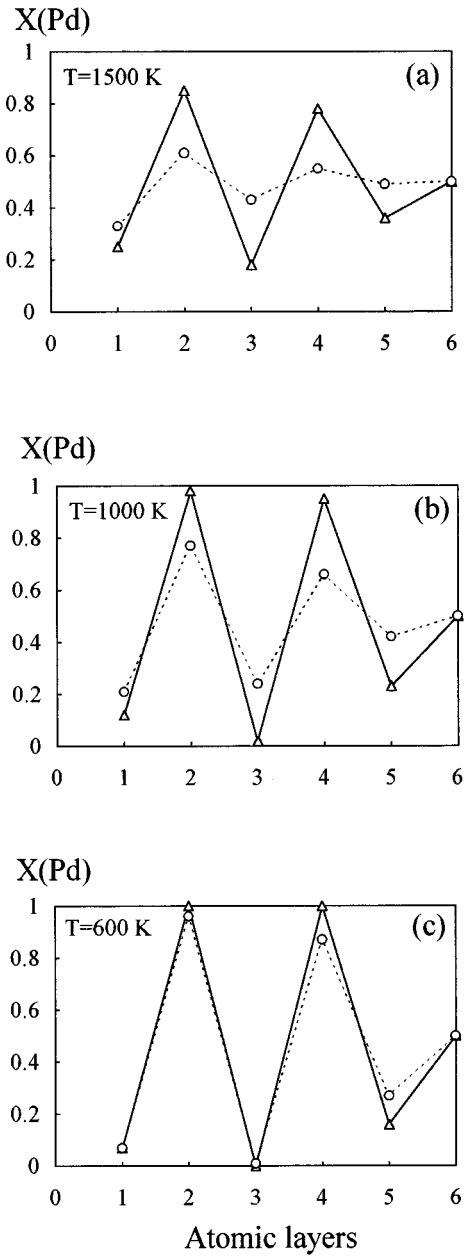

FIG. 14. Depth profiling of a (100) surface of a $Pd_{0.5}Cu_{0.5}$ alloy calculated for various temperatures and two different methods (see text). Triangles and circles represent, respectively, the results obtained with the basic model and with the equivalent medium approximation (EMA). (a) $T=1500$ K. (b) $T=1000$ K. (c) $T=600$ K.

there are changes in coordination. With respect to the top surface compositions, the agreement between theoretical and experimental results is generally good as has been discussed for a large number of fcc transition and noble metal alloys. The model has been applied also to Pt-Cu, Ag-Au, Cu-Ni, Au-Cu, and Pt-Ni bimetallic systems. The results agree well with the experimental results for all alloys except for Pt-Ni where we found a slight Ni segregation to the top layer instead of experimentally observed Pt segregation.

Concerning depth profiling, the consistency of our approach is discussed for the Pd-Cu (also Pt-Cu and Au-Cu) alloy, which exhibit order-disorder transitions. A convincing

coherence of the calculated profiles with bulk phase diagrams is found. Nevertheless, the disordered state assumption we use is not really justified for temperatures below T_c and a more rigorous approach would be required. Monte Carlo simulations could be a way to do so.

ACKNOWLEDGMENTS

We acknowledge the Indo French Center for the Promotion of Advanced Research, IFCPAR, for their financial assistance through Contract No. 806-2. We acknowledge gratefully Dr. Guy Treglia for helpful discussions. We acknowledge also Professor B. C. Khanra for a critical reading of the manuscript.

APPENDIX A

We list here relations between the A, p, q, and ξ parameters and the elastic constants or the equilibrium condition used to fit the TB-SMA parameters. The equilibrium condition is $12Ap=\sqrt{12}q\xi$:

$$C_{11}=\left(2p^2A+2pA+\frac{16q^2\xi}{12^{3/2}}-\frac{4q^2\xi}{12^{1/2}}-\frac{2q\xi}{12^{1/2}}\right)\Big/\Omega_0,$$

$$C_{44}=\left(p^2A+pA-\frac{2q^2\xi}{12^{1/2}}-\frac{q\xi}{12^{1/2}}\right)\Big/\Omega_0,$$

$$C_{12}=\left(p^2A+pA+\frac{16q^2\xi}{12^{3/2}}-\frac{2q^2\xi}{12^{1/2}}-\frac{q\xi}{12^{1/2}}\right)\Big/\Omega_0,$$

$$B=\tfrac{1}{3}(C_{11}+2C_{12}),$$

where Ω_0 is the atomic volume.

APPENDIX B

An expression of the surface free enthalpy and determination of the equilibrium state are given.

For the surface term the expression is more complex than these of the bulk since five layers are allowed to differ from the bulk in concentration. In addition the relaxation parameters have to be taken into account for the topmost layer. For clarity, only the free enthalpy of the first layer is explicitly derived:

$$\begin{aligned}
G_{\rm surf}=&(1+\delta_A)Z_L[\tfrac{1}{2}X_1^2\varepsilon_{AA}^0\Psi_{AA}(X_{1e})]+(1+\delta_A/2)Z_V\left[\frac{X_1X_2\varepsilon_{AA}^0[\Psi_{AA}(X_{1e})+\Psi_{AA}(X_{2e})]}{2}\right]\\
&+(1+\delta_B)Z_L[\tfrac{1}{2}(1-X_1)^2\varepsilon_{BB}^0\Psi_{BB}(X_{1e})]+(1+\delta_B/2)Z_V\left[\frac{(1-X_1)(1-X_2)\varepsilon_{BB}^0[\Psi_{BB}(X_{1e})+\Psi_{BB}(X_{2e})]}{2}\right]\\
&+(1+\delta_{AB})Z_L[X_1(1-X_1)\varepsilon_{AB}^0(X_{1e})\Psi_{AB}(X_{1e})]+[(1+\delta_A/2)Z_vX_1(1-X_2)+(1+\delta_B/2)Z_vX_2(1-X_1)]\\
&\times\left[\frac{[\varepsilon_{AB}^0(X_{1e})+\varepsilon_{AB}^0(X_{2e})]}{2}\,\frac{[\Psi_{AB}(X_{1e})+\Psi_{AB}(X_{2e})]}{2}\right]+\text{the contribution of the four other layers}\\
&+\sum_{i=1}^{5}RT[X_i\ln X_i+(1-X_i)\ln(1-X_i)].
\end{aligned}$$

We have to note that for the interactions between two adjacent layers i and $i+1$, the associated LJ potential term is the arithmetic mean, i.e.,

$$\Psi_{(X_{ie},X_{(i+1)e})}=\frac{\Psi_{(X_{ie})}+\Psi_{(X_{(i+1)e})}}{2}.$$

It is the same for ε_{AB}^0.

The equilibrium concentration is then found by minimizing the total free enthalpy: $G_{\rm tot}=G_{\rm surf}+G_{\rm bulk}$ with respect to X_i. So, $[\partial G_{\rm tot}/\partial X_i]$ must be equal to 0 for all $i\in[1,5]$. Since X_1, X_2, X_3, X_4, X_5, and X_b are dependent variables, we introduce the Lagrange multiplier method, which in fact leads to

$$i\in[1,5],[\partial G_{\rm surf}/\partial X_i]=[\partial G_{\rm bulk}/\partial X_b].$$

The quintuplet that minimizes the free energy is then determined numerically. It must verify the following inequality

$$\sum_{i=1}^{5}|([\partial G_{\rm surf}/\partial X_i]-[\partial G_{\rm bulk}/\partial X_v])|\leqslant\lambda,$$

where λ (nearly equal to 0) is a parameter that depends on the precision required.

*Author to whom correspondence should be addressed.

[1] P. Miegge, J. L. Rousset, B. Tardy, J. Massardier, and J. C. Bertolini, J. Catal. **149**, 404 (1994).
[2] J. C. Bertolini, J. L. Rousset, P. Miegge, J. Massardier, B. Tardy, Y. Samson, B. C. Khanra, and C. Creemers, Surf. Sci. **281**, 102 (1993).
[3] A. Rochefort, M. Abon, P. Delichère, and J. C. Bertolini, Surf. Sci. **294**, 43 (1993).
[4] J. L. Rousset, A. M. Cadrot, F. J. Cadete Santos Aires, A. Renouprez, P. Melinon, A. Perez, M. Pellarin, J. L. Vialle, and M. Broyer, J. Chem. Phys. **102**, 8574 (1995).
[5] N. H. Tsai, G. M. Pound, and F. F. Abraham, J. Catal. **50**, 200 (1977).
[6] F. F. Abraham and C. R. Brundle, J. Vac. Sci. Technol. **18**, 506 (1981).
[7] A. D. Van Langeveld and V. Ponec, Appl. Surf. Sci. **16**, 405 (1983).
[8] O. L. J. Gijzeman, Surf. Sci. **150**, 1 (1985).
[9] R. Hultgren, P. A. Desai, D. T. Hawkins, M. Gleiser, and K. K. Kelley, *Selected Values of the Thermodynamic Properties of Binary Alloys* (American Society of Metals, Metal Park, 1973).
[10] F. Cleri and V. Rosato, Phys. Rev. B **48**, 22 (1993).
[11] V. Rosato, M. Guillope, and B. Legrand, Philos. Mag. A **59**, 321 (1989).
[12] C. Kittel, *Introduction to Solid State Physics* (Wiley, New York, 1966).
[13] *Single Crystal Elastic Constants and Calculated Aggregated Properties*, edited by G. Simmons and H. Wang (MIT Press, Cambridge, 1971).
[14] W. R. Tyson and W. A. Miller, Surf. Sci. **62**, 267 (1977).
[15] M. Said, M. C. Desjonquères, and D. Spanjaard, Phys. Rev. B **47**, 4722 (1992).
[16] *Molecular Spectra and Molecular Structure Constants of Diatomic Molecules*, edited by K. P. Huber and G. Herzberg (Van Nostrand Reinhold, New York, 1979).
[17] K. Mukherjee, Philos. Mag. **12**, 302 (1965), and references cited therein.
[18] R. G. Donnely and T. S. King, Surf. Sci. **74**, 89 (1978).
[19] W. B. Pearson, *Handbook of Lattice Spacings and Structures of Metals and Alloys* (Pergamon, London, 1964).
[20] J. B. Darby, Jr. Myles, and K. M. Myles, Met. Trans. **3**, 653 (1972).
[21] G. N. Derry, C. B. McVey, and P. J. Rous, Surf. Sci. **326**, 59 (1995).
[22] A. D. Van Langeveld, H. A. C. M. Hendrickx, and B. E. Nieuwenhuys, Thin Solid Films **109**, 179 (1983).
[23] A. Noordermeer, G. A. Kok, and B. E. Nieuwenhuys, Surf. Sci. **172**, 349 (1986).
[24] J. Tersoff, Phys. Rev. B **42**, 10 965 (1990).
[25] D. G. Swartzfager, S. B. Ziemecki, and M. J. Kelly, J. Vac. Sci. Technol. **19**, 185 (1981).
[26] G. Hetzendorf and P. Varga, Nucl. Instrum. Methods Phys. Res. (to be published).
[27] F. J. Kuijers and V. Ponec, J. Catal. **60**, 100 (1979).